Pflügers Arch (1993) 422:523–529

Pflügers Archiv
European Journal of Physiology

Instruments and techniques

Intracellular pH in renal tubules in situ: single-cell measurements by confocal laserscan microscopy

M. Weinlich[1, 3], G. Capasso[2], and R. K. H. Kinne[3]

[1] Chirurgische Universitätsklinik Tübingen, Hoppe-Seyler-Str. 3, W-7400 Tübingen, Federal Republic of Germany
[2] Department of Pediatrics, First Faculty of Medicine, University of Naples, Naples, Italy
[3] Max-Planck-Institut für Systemphysiologie, Rheinlanddamm 201, W-4600 Dortmund 1, Federal Republic of Germany

Received July 17, 1992/Received after revision September 4, 1992/Accepted September 14, 1992

Abstract. Confocal laserscan microscopy with a dual-excitation device was used to record intracellular pH (pH_i) regulation in rat proximal convoluted tubules microperfused in vivo. Cells were loaded with the pH-sensitive, fluorescent dye 2′,7′-bis(carboxyethyl)-5(6)-carboxyfluorescein (BCECF). Single cells could be distinguished within the tubules and separate measurements were possible. Application of an NH_4Cl pulse by peritubular perfusion caused an immediate increase in intracellular pH. Intraluminal injection of NH_4Cl led to a slower increase in intracellular pH. In both cases, cessation of perfusion led to an immediate acidification. Peritubular perfusion with 300 μM 4,4′-diisothiocanato-dihydrostilbene-2,2′-disulphonic acid (H_2DIDS) caused an intracellular alkalinisation. Microperfusion, pH-sensitive dyes and confocal laserscan microscopy provide a new non-invasive method to measure intracellular pH effectively in individual cells of near-surface structures of the intact kidney.

Key words: Confocal microscopy – Fluorescence microscopy – Proximal tubule – 2′,7′-Bis(carboxyethyl)-5(6)-carboxyfluorescein – Intracellular pH – Viability – Rat

Introduction

To understand acid/base transport in the kidney, knowledge of intracellular pH (pH_i) regulation is essential. Owing to the complex pH_i regulation in the kidney (Alpern 1990; Aronson 1983), in vivo experiments are to be preferred. So far only a few methods allow measurement of pH_i in intact kidney. The use of pH-sensitive electrodes is very difficult and has a low success rate (Frömter 1984). Nuclear magnetic resonance measurements (Deutsch et al. 1984; Busa and Nuccitelli 1984) of intracellular pH cannot distinguish between the different cell types and the localisation of the kidney structures. Another method uses pH-sensitive fluorescent dyes together with an optical device (Roos and Boron 1981; Paradiso et al. 1987; Montrose et al. 1987; Musgrove et al. 1986). This microspectrofluorometry technique has been successfully used to measure pH_i changes non-invasively in kidney tubules in vivo (Alpern 1985; Alpern and Chambers 1986) and in vitro (Weiner and Hamm 1989). In the in vivo experiments tubules were loaded with pH-sensitive fluorescent dye 2′,7′-bis(carboxyethyl)-5(6)-carboxyfluorescein acetoxymethyl ester (BCECF-AM) and one whole loop of the tubule was used for microscopic recording. Even though new results were obtained by this method it still has several drawbacks. Out-of-focus fluorescence does contribute to the overall fluorescence signal. Different cell types, present in one loop, cannot be distinguished. Segments of fluorescent tubules that are not well perfused may also contribute to the fluorescence signal. Furthermore, long exposure of the loaded cells leads to photobleaching (Alpern 1985).

Confocal laserscan microscopy (Pawley 1990; Shotton 1989; White et al. 1987) offers the possibility to avoid the above-mentioned problems. Only signals from a thin confocal optical plane are registered. Therefore out-of-focus fluorescence is reduced significantly (Wang and Kurtz 1990). The contrast of the image is improved by a factor of 1.4 compared to conventional fluorescence microscopy (Wilson 1989). The use of highly sensitive photomultipliers leads to a reduction of overall light exposure and may therefore lower photobleaching.

In this paper a new method is described to measure single-cell pH_i changes in microperfused tubules in vivo by applying confocal laserscan microscopy with dual excitation and the pH-sensitive fluorescent dye BCECF. Single cells could be distinguished and differences in pH_i regulation could be registered. This method should allow to monitor changes in intracellular parameters of segments that contain various cell types, under conditions where the functional integrity of the epithelium or, in the case of microperfusion, the whole organ has been well maintained.

Correspondence to: R. Kinne

Materials and methods

Chemicals and solutions. A 10 mM stock solution of BCECF-AM ester (Molecular Probes, Eugene, Oro) in dimethylsulphoxide and a 10 mM stock solution of nigericin (Molecular Probes) in dimethylformamide/ethanol 3:1 were stored at −20° C. Inactin was from Promonta, FRG. 4,4′-Diisothiocyanatodihydrostilbene-2,2′-disulphonic acid (H_2DIDS; Molecular Probes) was added to the solutions at a final concentration of 1 mM. All other chemicals were from Sigma (St. Louis, Mo.). The infusion solution (Ringer solution) contained (in mM) 125 NaCl, 15 $NaHCO_3$, 4 KCl, 1.62 Na_2HPO_4, 0.38 NaH_2PO_4, 1 $MgCl_2$ and 1.5 $CaCl_2$. In NH_4Cl-containing solutions Na^+ was replaced by NH_4^+. The calibration solution with high K^+ contained (in mM) 140 KCl, 2 K_2HPO_4, 1 $MgSO_4$, 1 $CaCl_2$, 10 glucose, 10 HEPES and 10 μM nigericin. pH was adjusted using *N*-methyl-D-glucamine.

Proximal tubules in vivo. Experiments were done on male Wistar rats (200−250 g body weight). They were anaesthetized by intraperitoneal injection of Inactin (120 mg/kg body weight), tracheostomized, placed in the right lateral position on a heated table and prepared for micropuncture (Capasso et al. 1985). The left jugular vein was cannulated with Pe-50 tubing and used for infusion via a syringe pump of 0.9% saline at 2.2 ml/h. Rectal temperature was measured. The left kidney was exposed through a flank incision, made free of perirenal fat and immobilized in a lucid chamber by using 3% agar in 0.9% saline. The last portion of the proximal tubule (S_2 segment) was identified by inserting a pipette (5.5 μm outer diameter, o.d.) containing 0.07% FD & C blue dye dissolved in end-proximal Ringer solution. Peritubular capillaries were perfused with a micropipette (9−10 μm o.d.). The area of the punctured capillary and the perfused cortex was approximately 300 μm in diameter.

Loading tubules with BCECF. A luminal perfusion pipette (7−8 μm o.d.) containing 40 μM BCECF-AM dissolved in Ringer solution, without blue dye, was inserted in one of the last accessible loops of the proximal tubule. Tubular cells were loaded with the fluorescent dye, which was immediately diluted in the perfusate by the free-flow conditions. BCECF-AM is the membrane-permeant acetoxymethyl ester of BCECF. Intracellular esterases cleaved BCECF-AM into its fluorescent, membrane-impermeant form (Thomas et al. 1979; Tsien 1989). This manoeuver usually lasted 10−15 min until a sufficient fluorescence signal was visible. Tubules were allowed to rest for 30 min to compensate for any disturbance due to dye loading.

Confocal laserscan microscopy. The confocal system used consisted of an MRC-500 confocal imaging system (Bio-Rad, Boston, Ma.) and a Nikon Labophot epifluorescence microscope. The excitation light at 488 nm was provided by an argon ion laser (Ion Laser Technology, U). A second helium/cadmium laser (Liconix) was adapted to the confocal laserscan microscope for excitation at 442 nm (Opitz et al. 1991), using mirrors on an optical bench. To avoid photobleaching a 1% neutral-density filter was used. This reduced the laser power from about 10 W at 488 nm to 100 mW. The laser beams were scanned by two galvanomeric mirrors in a raster pattern across the surface of the tissue. The fluorescence signal emitted by the excited dye was collected by the objective and descanned by the same galvanometric mirrors, passing an emission filter (OG 515 LP) and the variable confocal pinhole. The fluorescence signal was measured by a photomultiplier. The digitalized photomultiplier output was collected on a Nimbus AX personal computer. A special program was designed to collect fluorescence data in set time intervals and store picture frames on hard disk. Further data processing was performed using the Bio-Rad software.

A ×6.3 objective (Leitz, Wetzlar, FRG) with a numerical aperture of 0.20 was used. To determine the depth of field of the optical set-up (Brakenhoff et al. 1979) very small fluorescent beads (0.6 μm) were sectioned at consecutive focus levels. The relative intensity measured at 488 nm excitation, plotted against the distance of the focus from the bead, yields a bell-shaped curve (Fig. 1). The depth of focus of this set-up is described with ΔZ, which is the distance of the focus from the bead at half-maximum intensity. The measured value is 9.5 μm. Even with a partially opened pinhole the confocal arrangement does reflect more flare and scattered light than a conventional light microscope (Carrington et al. 1990).

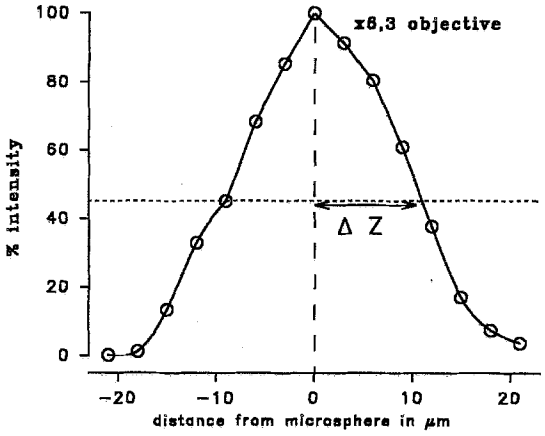

Fig. 1. Determination of the depth of field of the ×6.3 objective with a numerical aperture of 0.20. A fluorescent bead with a diameter of 0.6 μm was optically sectioned at consecutive focus levels with 488 nm excitation. The depth of focus is described with ΔZ, which is the distance of the focus from the bead at half-maximum intensity. The measured value was 9.5 μm

For estimation of the confocal plane thickness of the objective the following formula was applied (A. Siegel, Carl Zeiss Laboratories, Oberkochen, FRG, personal communication):

$$\Delta Z = 0.89\, n\lambda/(\mathrm{NA})^2$$

where ΔZ is the distance of the focus at half-maximum intensity, n is the refractive index, λ is the excitation wavelength and NA is the numerical aperture of the objective. The calculated estimate for ΔZ was 10.9 μm.

For intracellular pH calculations, the grey-level image obtained at 488 nm excitation (pH-dependent wavelength) was divided by the 442-nm excitation image (pH-independent). The resulting grey-level image was the so-called ratio image, which indicated changes of intracellular pH. To calculate the absolute pH_i, separate calibration experiments were performed (Alpern 1985). The tubules were perfused on the luminal and periluminal side with high-potassium solutions containing nigericin at pH 6.8, 7.2 and 7.6. The calibration curve obtained from these experiments was used for calculation of the absolute intracellular pH.

At the beginning of each experiment autofluorescence was measured. After dye loading the photomultiplier sensitivity was set just above the autofluorescence level to subtract any background signal. The highest fluorescence intensity measured was set to about 200 on a grey-level scale ranging from 0 to 255 and never reached 255 during the experiment.

The viability of every single cell could be directly monitored using the intracellular distribution of BCECF. The dye is more concentrated in the nucleus than in the cytoplasm of viable cells (Wang and Kurtz 1990; Rosenberg et al. 1991; Bright et al. 1987). This accumulation is partially an active ATP-dependent process (Allen et al. 1990). The loss of cell viability is accompanied by a decrease in the fluorescence intensity in the nucleus. Dead cells have a dark nucleus and can be stained with trypan blue. Confocal microscopy allows the direct, quantitative monitoring of dye distribution, because of the narrow depth of field. Distribution of fluorescence intensities of BCECF in viable cells can be expressed by the formula:

$$I_{nuc} > I_{cyt}$$

I_{nuc} is the fluorescence intensity of BCECF, excited at 442 nm, in the nucleus and I_{cyt} is the fluorescence intensity of BCECF in the cytoplasm.

Changes in the position of the cells in a confocal microscope in the axial direction (z direction) lead to stronger intensity changes than in a conventional microscope, because of the narrow depth of field (Fig. 1). Drastic changes of the fluorescence intensities of more than 50% caused artificial alterations of the ratio of more than 20% (Weinlich et al. in press). To reduce, in the in vivo experiments, the influence of kidney movement by respiration, arterial pulsations or artificial movement, the fluorescence intensity at 442 nm excitation was measured and all experiments with an intensity change of more than 50% were excluded. Another criterion was the digital image. Experiments with drastic changes in the shape or location of the tubules were considered as invalid.

Statistical analysis. Results are expressed as means ± SEM. Statistical significance was evaluated by a paired Student's t-test. A p value <0.05 was considered significant.

Results

Loading

Before the experiment was started the tubules were examined in bright field and epifluorescence (Fig. 2). No change in size or morphology was visible after loading. The diameter of the tubules did not change and the dye did not penetrate to neighbouring tubules. Single tubular cells could be distinguished. The extent of loading in the loop decreased with the distance from the injection side. Analysis of fluorescence intensity of the cells revealed a decrease in dye loading from proximal to distal parts of the loop (Fig. 2).

In four experiments a distal tubule was loaded with BCECF. The segments showed well loaded cells; in some parts of the segments single cells could be distinguished (Fig. 3).

Control experiments

Steady state. Fluorescence signals were collected over a 5-min period. The steady decrease of overall fluorescence at 442 nm excitation was between 7% and 10% in 5 min. $t_{1/2}$ was calculated to be 35–50 min. The ratio did not change significantly within this period. The steady-state pH_i was 7.28 ± 0.06 ($n = 20$).

Injection of plain infusion solution. Infusion solution was injected peritubularly (Fig. 4) or intraluminally to detect any artifical changes of the ratio due to movement or changes of composition of the environment of the tubules. An 80 s injection did not lead to any significant change in the ratio during or after the injection.

Calibration

Calibration was performed by simultaneous peritubular and intraluminal injection of nigericin-containing high-potassium solutions. Because of the complicated procedure, separate calibration experiments had to be performed. Calibration solutions were adjusted to pH 6.80, 7.20 and 7.60 and the three different pH values of the solutions were plotted against the measured ratios (Fig. 5). A regression curve was calculated with the equation $y = 1.16\,x - 7.46$ ($p < 0.05$). This equation was used to convert the ratios from the other experiments to absolute pH values.

NH_4Cl pulse

Peritubular injection. Fast intracellular pH changes were induced by injecting 25 mM NH_4Cl buffer into a peritubular capillary (Fig. 6) for 50 s. At the beginning of the injection an immediate increase in intracellular pH from 7.24 ± 0.04 (SEM, $n = 4$) to 7.51 ± 0.07 was observed. Within a period of 50 s the signal almost dropped to the baseline level. Stopping the injection after 50 s led to an immediate decrease in intracellular pH to 7.15 ± 0.03. Recovery of intracellular pH to almost the baseline level was seen in the following minute.

Separate measurements in different areas of interest were made of segments of tubules that were reached by the peritubular injection and segments that were not reached. Only tubular segments that had a good peritubular perfusion with NH_4Cl showed the rapid alkalinisation. Other segments stayed at the baseline level (Fig. 7). These different responses were also seen in other experiments with peritubular injection.

Intraluminal injection. Intraluminal injection of 25 mM NH_4Cl caused a steady increase in intracellular pH from 7.29 ± 0.02 to 7.52 ± 0.06 after 40 s (Fig. 8). After NH_4Cl exposure the intracellular pH dropped immediately to 7.20 ± 0.02. A recovery of intracellular pH within 1 min after the injection could be observed.

In some experiments signals directly taken from the injection site led to questionable results. Fluorescence intensities and the size of the tubule changed significantly at this location. Better pH responses were obtained about 30 µm distal from the injection site.

Peritubular injection of H_2DIDS

Injection of 300 µM H_2DIDS on the peritubular side for 80 s caused an increase in intracellular pH from 7.26 ± 0.07 to 7.42 ± 0.05 within 20 s (Fig. 9). Until the end of H_2DIDS injection the intracellular pH stayed at the elevated level. After termination of the injection, the intracellular pH dropped back to the baseline level.

Discussion

Combination of the pH-sensitive fluorescent dye BCECF with a dual-excitation confocal laserscan microscope allowed measurements of the intracellular pH of near-surface proximal tubules. Peritubular exposure to NH_4Cl showed an immediate alkalinisation of the epithelial cells,

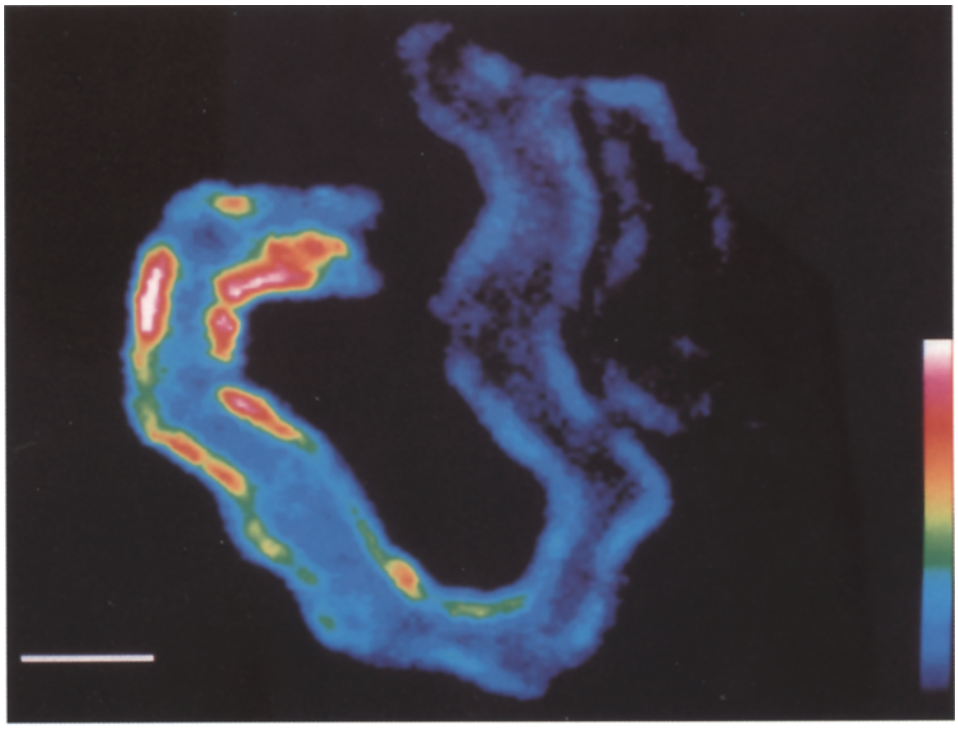

Fig. 2. Proximal tubule loaded with 2′,7′-bis(carboxyethyl)-5(6)-carboxyfluorescein (BCECF) viewed with confocal laserscan microscopy (excitation 442 nm). A decrease in fluorescence intensity from injection site to distal parts of the loop can be seen. Single cells can be distinguished. *Scale bar* is 50 μm

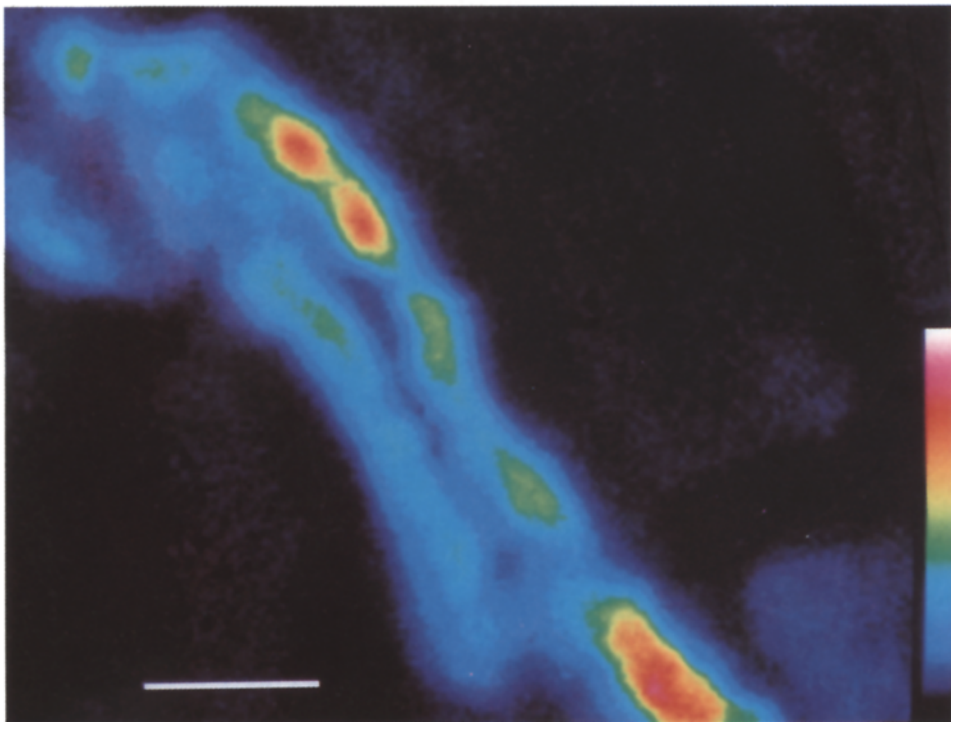

Fig. 3. Distal tubule loaded with BCECF (excitation 442 nm). Strong fluorescence inside single cells is visible. The lumen of the distal tubule is almost free of fluorescence because of the effect of the confocal plane. *Scale bar* is 25 μm

due to a fast entry of ammonia into the cells (Roos and Boron 1981). This alkalinisation slowly decreased through the slow entry of NH_4^+ and the effect of intracellular pH-regulatory systems. After the exposure, the expected acidification, caused by an exit of ammonia from the cells, occurred. A different intracellular pH response was observed after luminal NH_4Cl perfusion. A steady increase in intracellular pH was observed, which lasted 40 s until maximum alkalinisation was reached. These findings can be explained by a relatively low permeability of the apical membrane to NH_3 (Kikeri et al. 1989). NH_3 entry is dependent on the area and composition of the membrane. Even though the apical surface area is about four times larger than the basolateral surface area (Pfaller et al. 1985), which would cause a higher entry of NH_3 from the apical side into the cell, the permeability could be significantly lower. The lipid composition and the protein-to-lipid ratio of the two membranes differs

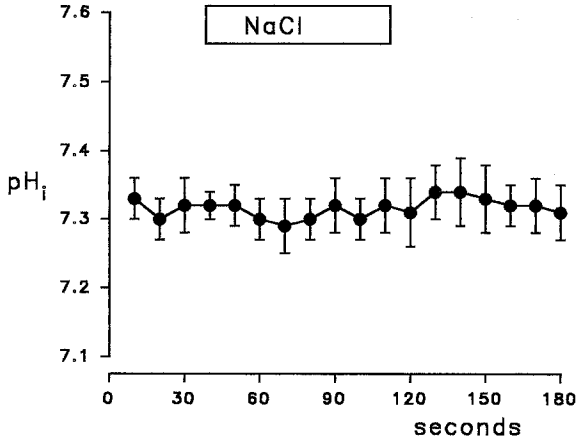

Fig. 4. Peritubular injection of plain infusion solution. To determine the effect of infusion solution on the intracellular pH measurement, plain infusion solution was injected peritubularly. A significant change in intracellular pH was not observed ($n = 4$)

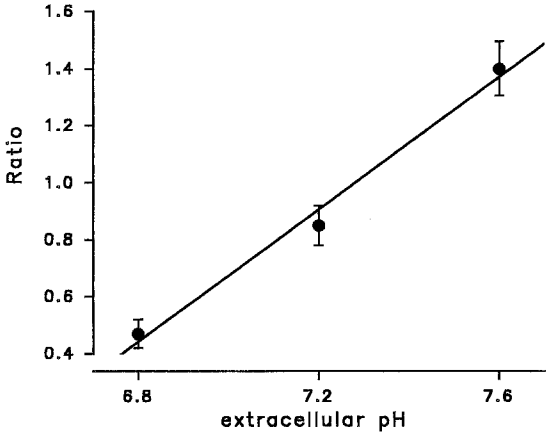

Fig. 5. Calibration curve. Calibration was performed by peritubular and intraluminal injection of nigericin-containing high-potassium solution. A linear regression curve could be fitted through the calibration values ($y = 1.16\,x - 7.46$; $P < 0.05$, $n = 3$)

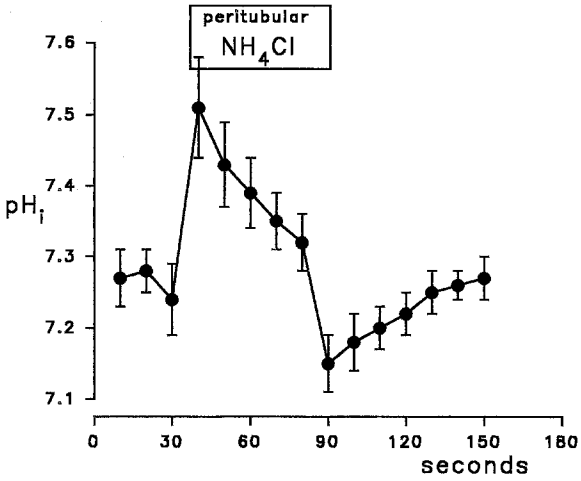

Fig. 6. Time course of H_i changes during injection of 25 mM NH_4Cl buffer in the peritubular capillary of a proximal tubule for 50 s. An immediate increase in intracellular pH could be observed. After removal of NH_4Cl an acidification of the cells occurred ($n = 4$)

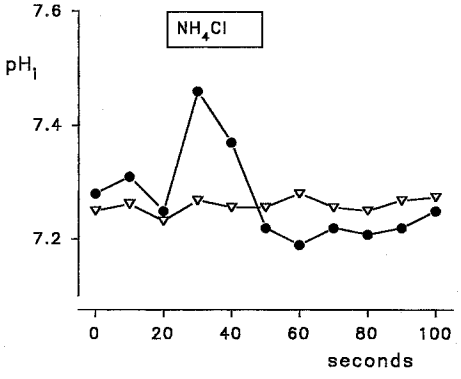

Fig. 7. Dependence of intracellular pH response on the quality of peritubular NH_4Cl perfusion. Only well-perfused parts of the investigated tubule showed an adequate intracellular pH increase after NH_4Cl perfusion. (▽ = not perfused; ● = well perfused)

(Golchini and Kurtz 1988; Kinne and Kinne-Saffran 1992), which could explain this lower permeability. Another explanation might be a secretion of NH_3 or a passive back-flux of NH_4^+ (Garvin et al. 1987). The Na^+-K^+-$2Cl^-$ cotransporter is able to take NH_4^+ up into the cells, at least in thick ascending limb cells (Kinne et al. 1986). These different transport systems may also contribute to the changed intracellular pH behaviour with luminal NH_4Cl exposure.

Peritubular H_2DIDS blocked the elimination of bicarbonate, leading to more alkaline cells. This is in agreement with work by Alpern, who explained this alkalinisation by an inhibition of a Na-HCO_3 cotransport mechanism, which is responsible for 90% of basolateral HCO_3 permeability (Alpern and Chambers 1986; Alpern 1990).

Compared to other possibilities of intracellular pH measurement in tubules in vivo, like pH-sensitive electrodes (Yoshitomi and Frömter 1984) or microspectrofluorometry (Alpern 1985; Alpern and Chambers 1986),

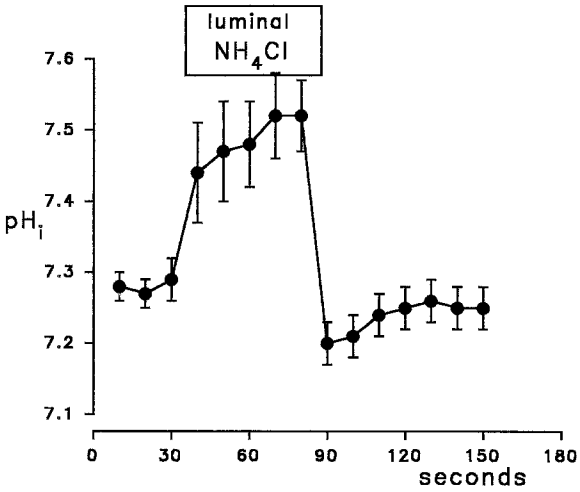

Fig. 8. Intraluminal injection of 25 mM NH_4Cl into proximal tubules for 50 s. A steady increase in intracellular pH was measured. Stopping NH_4Cl injection led to an immediate intracellular acidification ($n = 4$)

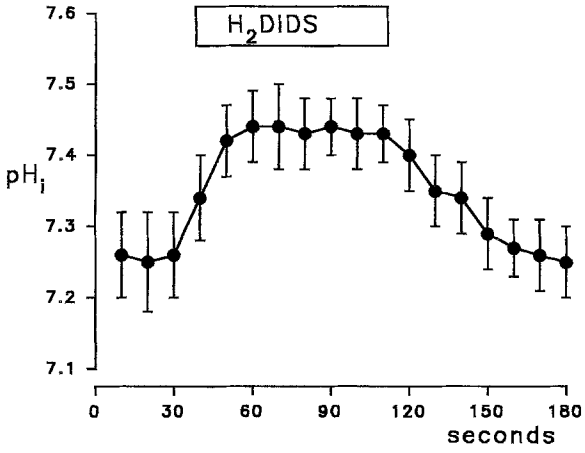

Fig. 9. Peritubular injection of 300 μM H_2DIDS 4,4′-diisothiocyanatodihydrostilbene-2,2′-disulphonic acid led to an elevation in intracellular pH of 0.26 pH unit. After termination of the injection the intracellular pH dropped back to the baseline level ($n = 4$)

confocal laserscan microscopy does have the following advantages and disadvantages.

In experiments in vivo the surface structures of the kidney move as a result of respiration, arterial pulsation or experimental manipulations. Confocal laserscan microscopy allows an immediate view of the fluorescence intensity image and therefore an evaluation of the degree of movement during the experiment. Movement in the x, y direction could easily be compensated by moving the area of interest on the digital image. Movement in the z direction with a confocal laserscan microscope leads to a stronger reduction of the fluorescence intensities, compared to microspectrofluorometry, because of the confocal optical behaviour. In these experiments the confocal plane thickness for the × 6.3 objective was 9.5 μm. Movement of the cell by 9.5 μm in the z direction will, therefore, lead to a decrease in fluorescence intensity by 50%. In the confocal laserscan microscope the drastic decrease in both emission intensities (excited with 488 nm and 442 nm) leads to an artificial change in the ratio (Weinlich et al. 1992), as a result of a non-linear relationship between the fluorescence intensity measured by the photomultiplier and the grey-level intensity value of the digital image. Only in the case of stable conditions with little motion can the deviation from a linear relationship be neglected.

Movement of the cells was the major problem in using confocal laserscan microscopy in comparison to conventional fluorescence microscopy. In moving tissue it was necessary to find a compromise between high-resolution (narrow depth of field) and artefacts due to movement. In this set-up the × 6.3 objective with a numerical aperture of 0.20 gave the best results. Another drawback of confocal laserscan microscopy is the limitation of the laser light to a distinct wavelength. A combination of dyes or the use of other pH-sensitive dyes would require additional laser sources or filter changes.

The resolution of the confocal image is about 1.4 times higher than that of a conventional image (Wilson 1989). Confocal laserscan microscopy reduces the signal collection in the z direction (White et al. 1987). Therefore single cells in the tubule were emphasized and fluorescence signals reduced from above or below a cell in focus. In heterogeneous tissue, like the distal tubule, this function may help to differentiate between different cellular pH responses.

Measurement of the ratio of the digital image within different areas of interest helped to distinguish between well-perfused and badly perfused segments of the tubules. In peritubular perfusion not all parts of the tubule are well perfused. Even though a bright-field view of the perfused region helped to select the well-perfused segments, a functional proof assures the selection of the adequate segment. In intraluminal perfusion experiments intracellular measurements close to the injection site were rich in artefacts.

Confocal laserscan microscopy improves conventional microspectrofluorometry (White et al. 1987). Out-of-focus fluorescence signals can be reduced (Wang and Kurtz 1990), because of the thin confocal plane, allowing single-cell imaging. This technology thus opens new possibilities to measure intracellular pH in cells in intact tubules as well as in other epithelia composed of a variety of cells. The high resolution of confocal microscopy allows the detection of fluorescence changes in single cells and even in subcellular compartments.

Acknowledgements. We thank Ms. Theiss for her excellent technical assistance. G. Capasso was supported by the Italian Research Council (grant 89.02468.04). M. Weinlich was supported by the Deutsche Forschungsgemeinschaft (WE 1362/1-1).

References

Allen CN, Harpur ES, Gray TJB, Simmons NL, Hirst BH (1990) Efflux of bis-carboxyethyl-carboxyfluorescein (BCECF) by a novel ATP-dependent transport mechanism in epithelial cells. Biochem Biophys Res Commun 172:262–267

Alpern RJ (1985) Mechanism of basolateral membrane $H^+/OH^-/HCO_3^-$ transport in the rat proximal convoluted tubule. J Gen Physiol 86:613–636

Alpern RJ (1990) Cell mechanisms of proximal tubule acidification. Physiol Rev 70:79–114

Alpern RJ, Chambers M (1986) Cell pH in the rat proximal convoluted tubule. Regulation by luminal and peritubular pH and sodium concentration. J Clin Invest 78:502–510

Aronson PS (1983) Mechanisms of active H^+ secretion in the proximal tubule. Am J Physiol 245:F647–F659

Busa WB, Nuccitelli R (1984) Metabolic regulation via intracellular pH. Am J Physiol 246:R409–R438

Brakenhoff GJ, Blom P, Barends P (1979) Confocal scanning light microscopy with high aperture immersion lenses. J Microsc 117:219–232

Bright GR, Fisher GW, Rogowska J, Taylor DL (1987) Fluorescence ratio imaging microscopy: temporal and spatial measurements of cytoplasmic pH. J Cell Biol 104:1019–1033

Capasso G, Kinne-Saffran E, De Santo NG, Kinne R (1985) Regulation of volume reabsorption by thyroid hormones in the proximal tubule of rat: minor role of luminal sodium permeability. Pflügers Arch 403:97–104

Carrington WA, Fogarty KE, Lifschitz L, Fay FS (1990) Three dimensional imaging on confocal and wide-field microscopes. In: Pawley J (ed) Handbook of biological confocal microscopy. Plenum, New York, pp 151–161

Deutsch C, Taylor JS, Price M (1984) pH homeostasis in human lymphocytes: modulation by ions and mitogen. J Cell Biol 98:885–893

Frömter E (1984) Viewing the kidney through microelectrodes. Am J Physiol 247:F695–F705

Garvin JL, Burg MB, Knepper MA (1987) NH_3 and NH_4^+ transport by rabbit renal proximal straight tubules. Am J Physiol 252:F232–F239

Golchini K, Kurtz I (1988) NH_3 permeation through the apical membrane of MDCK cells is via a lipid pathway. Am J Physiol 255:F135–141

Kikeri D, Sun A, Zeidel ML, Hebert SC (1989) Cell membranes impermeable to NH_3. Nature 339:478–480

Kinne R, Kinne-Saffran E (1992) Renal plasma membranes: isolation, general properties, and biochemical components. In: Windhager EE (ed) Handbook of physiology: renal physiology. Oxford University Press, New York, pp 2083–2117

Kinne R, Kinne-Saffran E, Schütz H, Schölermann B (1986) Ammonium transport in medullary thick ascending limb of rabbit kidney. Involvement of the Na^+,K^+,Cl^- cotransporter. J Membr Biol 94:279–284

Montrose MH, Friedrich T, Murer H (1987) Measurements of intracellular pH in single LLC-PK1 cells: recovery from an acid load via basolateral Na^+/H^+ exchange. J Membr Biol 97:63–78

Musgrove E, Rugg C, Hedley D (1986) Flow cytometric measurement of cytoplasmic pH: a critical evaluation of available fluorochromes. Cytometry 7:347–355

Opitz N, Weinlich M, Mooren F, Keinemann F-K, Kinne R (1991) Dual wavelength excitation in confocal laser scanning microscopy: intracellular pH measurements with a fluorescent indicator. Biomed Technik 36:132–133

Paradiso AM, Tsien RY, Demarest JR, Machen TE (1987) Na-H and Cl-HCO_3 exchange in rabbit oxyntic cells using fluorescence microscopy. Am J Physiol 253:C30–C36

Pawley J (1990) Handbook of biological confocal microscopy. Plenum, New York

Pfaller W, Gstraunthaler G, Kotanko P (1985) Compartments and surfaces in renal cells. In: Kinne RKH (ed) Renal biochemistry. Cells, membranes, molecules. Elsevier, Amsterdam, pp 1–62

Roos A, Boron WF (1981) Intracellular pH. Physiol Rev 61:296–434

Rosenberg SO, Berkowitz PA, Li L, Schuster VL (1991) Imaging of filter-grown epithelial cells: MDCK Na^+-H^+ exchanger is basolateral. Am J Physiol 260:C868–C876

Shotton DM (1989) Confocal scanning optical microscopy and its applications for biological specimens. J Cell Sci 94:175–206

Thomas JA, Buchsbaum RN, Zimniak A, Racker E (1979) Intracellular pH measurements in Ehrlich ascites tumor cells utilizing spectroscopic probes generated in situ. Biochemistry 18:2210–2218

Tsien RY (1989) Fluorescent indicators of ion concentrations. Methods Cell Biol 30:127–156

Wang X, Kurtz I (1990) H^+/base transport in principal cells characterized by confocal fluorescence imaging. Am J Physiol 259:C365–C373

Weiner ID, Hamm LL (1989) Use of fluorescent dye BCECF to measure intracellular pH in cortical collecting tubule. Am J Physiol 256:F957–F964

Weinlich M, Capasso G, Kinne RKH (1992) Confocal microscopy. In: Giebisch G, Ussing HH, Kristensen P (eds) Membrane transport in biology, vol 6 (in press)

White JG, Amos WB, Fordham M (1987) An evaluation of confocal versus conventional imaging of biological structures by fluorescence light microscopy. J Cell Biol 105:41–48

Wilson T (1989) Trends in confocal microscopy. Trends Neurosci 12:486–493

Yoshitomi K, Frömter E (1984) Cell pH of rat renal proximal tubule in vivo and the conductive nature of peritubular HCO_3^- (OH^-) exit. Pflügers Arch 402:300–305